EPSC Abstracts
Vol. 13, EPSC-DPS2019-166-1, 2019
EPSC-DPS Joint Meeting 2019

EPSC
EPSC-DPS Joint Meeting 2019
15–20 September 2019 | Geneva, Switzerland

Atmosphere-Interior Exchange on Magma Planets

Edwin S. Kite (1), Bruce Fegley Jr. (2), Laura Schaefer (3), Eric Gaidos (4). (1) University of Chicago (kite@uchicago.edu) (2) Washington University in St. Louis (3) Stanford University (4) University of Hawaii.

Abstract.

Many short-period rocky exoplanets have dayside magma pools [1-3]. We provide estimates of magma-planet outgassing rates and magma composition. Pool-surface composition is set by the competing effects of fractional vaporization (→ evolved composition) and surface-interior exchange (→ reset to primitive composition) (Fig. 1). We use basic models to explore the controls on the rate of surface-interior exchange. We find:- (1) atmosphere-interior exchange is fast enough to buffer surface composition (likely low albedo) when the planet's bulk-silicate FeO concentration is low, and slow when FeO concentration is high; (2) magma pools are compositionally well-mixed for substellar temperatures $\lesssim$2400 K, but compositionally patchy and rapidly variable for substellar temperatures $\gtrsim$2400 K; (3) magma currents within the magma pool cool the base of the magma pool ("tectonic refrigeration"), so the usual upper boundary condition for modeling the solid-mantle circulation of hot rocky exoplanets is too warm. (This abstract is updated from an LPSC abstract by the same authors; details of our study can be found in ref. [18]).

1. Background.

Over one hundred exoplanets are likely magma planets (e.g. CoRoT-7b, Kepler-10b, WASP-47e; TOI-402.01 is marginal) [4-6]. These molten surfaces are tantalizing because they are relatively easy to detect and characterize [1-3] - what sets molten-surface composition? The melt-coated dayside is exposed to intense insolation, sufficient to remove H_2 [7] and to maintain a thin silicate atmosphere [8] (Fig. 1). The most-volatile rock-forming element constituents of the melt (e.g. Na, K, Fe) preferentially partition into the atmosphere. These atmospherically transported volatiles are cold-trapped on the permanent nightside, or lost to space (Fig. 1). If trans-atmospheric distillation is faster than mass exchange between the melt pool and the solid interior, then surface composition will differ from bulk-planet silicate composition (possibly evolving to high-albedo ceramic). But if mass exchange between the melt pool and solid interior is fast, then surface composition will be repeatedly reset towards bulk-planet silicate composition (and, presumably, low albedo).

In the first (compositionally evolved) case, with relatively slow atmosphere-interior exchange, preferential loss of volatiles (Na, K, Fe ...) creates a refractory Ca-Al-rich lag [9]. The lag armors the vulnerable volatile-rich interior, as on a comet. After lag formation, atmospheric pressure will be everywhere $\lesssim O(1)$ Pa. In the second (compositionally buffered) case, Na, K, and Fe are replenished by surface-interior exchange; the exosphere fills with Na and K; and surface compositional evolution is extremely slow: it is buffered by the whole planet's silicate mass.

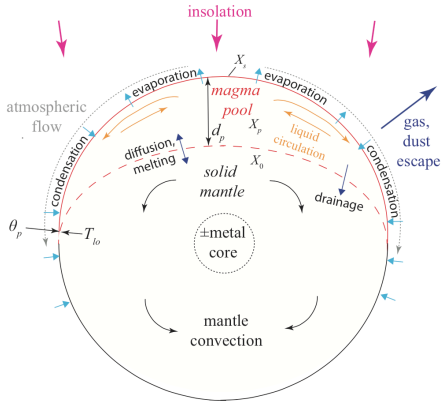

Fig. 1. *Processes shaping the surface composition of a hot rocky exoplanet. Magma pool (depth d_p, mean composition X_p, surface composition X_s) overlies a solid mantle (composition X0). d_p is shown greatly exaggerated. Tlo corresponds to the lock-up temperature that defines the edge of the melt pool. θ_p corresponds to the angular radius of the melt pool.*

To what extent does fractional evaporation drive the hot rocky exoplanets' dayside surface composition? We set out to determine the rates of surface-atmosphere versus surface-interior exchange. To do this, we quantify the key controls on magma pool surface composition (Fig. 1): stirring of the melt pool, chemical distillation of the pool through atmospheric flow, and (crucially) the buoyancy evolution of melt pools undergoing fractional evaporation (Fig. 2).

2. Model.

In order for surface composition to deviate from pool-average composition (Fig. 1), the ocean mixing timescale τ_T must be shorter than the time (τ_X) needed for evaporatic ablation by fractional vaporization (advection). We use simple scalings for the ocean overturning circulation [10]. To find the fractional vaporization rate, we need a model of the winds, which

we adapt from vertically-averaged models of Io's sublimation-driven atmosphere [11,12]. The ratio τ_X/τ_T decreases with temperature because evaporation increases much more quickly with temperature than thermal diffusion in the liquid. (Thermal diffusion in the liquid is needed to drive upwelling in horizontal-circulation). Neither winds nor currents much affect surface energy balance (for $T \lesssim$ 3000K). Next, we use the MAGMA code [8,13], plus literature equations-of-state [14], to see if the density of the chemically-fractionated reservoir (the residual magma left behind during fractional evaporation) is less than initial density throughout fractional evaporation. This determines whether surface magma will sink (Fig. 2).

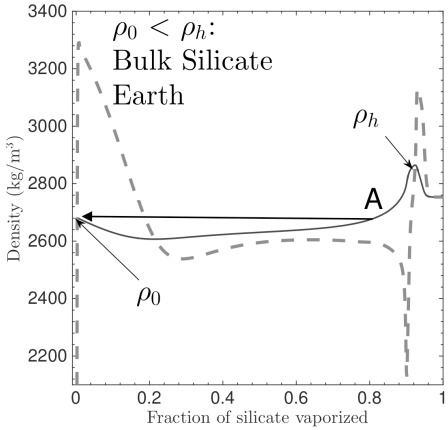

Fig. 2. Density evolution for fractional vaporization (at 2000K) of an initial Bulk-Silicate-Earth composition. Thin black solid curve corresponds to the density of residual magma, and thick gray dashed curve corresponds to the density-upon-condensation of the gas. At point A, the surface boundary layer sinks into the interior. ρ_h corresponds to the maximum density at >70 wt % fractional vaporization. ρ_0 corresponds to unfractionated magma density.

3. Results and tests

Results are summarized in Fig. 3. Magma-pool overturning circulation and differentiation can be viewed as a new tectonic mode for rocky planets at temperatures too high for plate tectonics, stagnant-lid convection, or heat-pipe recycling. Surface-interior exchange on magma planets is driven by near-surface contrasts in melt density (and can shut down if the surface layer becomes stably buoyant). In turn, these density effects are regulated by two factors (Fig. 3). (1) Relative vigor of winds and currents. For substellar temperature $\lesssim$2400K ("ocean-dominated" worlds), magma-pool overturning circulation outruns net evaporation, and pool surface composition tracks bulk pool composition. For substellar temperature $\gtrsim$2400K ("atmosphere-dominated" worlds), pool overturning circulation is slow compared to atmospheric transport, and fractional evaporation drives pool composition away from the composition of the bulk of the pool. (2) A second factor is exposure of the planet's building-blocks to H_2O, which affects the bulk silicate FeO content. This second effect is discussed in detail in [18]. In future, magma composition may be constrained using atmospheric column densities of Na and K [15], surface spectra [16], and the properties of material streaming from disintegrating magma planets such as K2-22b [17,19]. This may constrain magma planet migration distances [20].

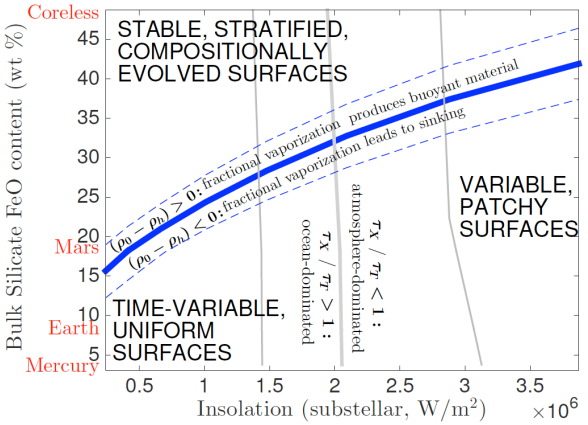

Fig. 3. Magma planet phase diagram. Stratification index (ρ_0 - ρ_h) is contoured at +50 kg/m^3 (top dashed blue line), 0 kg/m^3 (thick solid blue line), and -50 kg/m^3 (bottom dashed blue line). Planets below the line are unlikely to have CaO/Al_2O_3-dominated surfaces, planets above the line are likely to have CaO/Al_2O_3-dominated surfaces. Ocean-dominance index τ_X/τ_T is contoured at 10 (left gray line), 1 (thick gray line), and 0.1 (right gray line), for 50 wt% vaporization. Lower-left quadrant corresponds to magma pools with uniform, but time-variable surfaces, well-stirred by currents (low albedo?). Lower-right quadrant corresponds to atmosphere-dominated magma pools with variable, patchy surfaces driven by evaporative overturn. Upper two quadrants correspond to planets with stable, stratified, CaO/Al_2O_3-dominated surfaces (high albedo?). Calculations assume planet period 0.84 days, radius 1.5× Earth, and gravity 1.9× Earth (= Kepler-10b).

References: [1] Rouan et al. (2011) *ApJ*. [2] Demory (2014) *ApJ*. [3] Sheets & Deming (2017) *ApJ*. [4] Leger et al. (2009) *A&A*. [5] Batalha et al. (2011) *ApJ*. [6] Dai et al. (2015) *ApJ*. [7] Lopez & Fortney (2014) *ApJ*. [8] Schaefer & Fegley (2009) *Icarus*. [9] Leger et al. (2011) *Icarus*. [10] Vallis, *Atmospheric & Oceanic Fluid Dynamics*. [11] Ingersoll (1989) *Icarus*. [12] Castan & Menou (2011) *ApJ*. [13] Fegley & Cameron (1987) *EPSL*. [14] Ghiorso & Kress (2004) *Am. J. Sci.* [15] Heng et al. (2015) *ApJ* [16] Samuel et al. (2014) *A&A* [17] Budaj et al. (2015) *MNRAS*. [18] Kite et al. (2016) *ApJ*. [19] Vidotto et al. (2019) *MNRAS*. [20] Dai et al. (2018) *ApJL*.